Journal of Organometallic Chemistry 846 (2017) 208–216

Contents lists available at ScienceDirect

Journal of Organometallic Chemistry

journal homepage: www.elsevier.com/locate/jorganchem

Mononuclear half-sandwich iridium and rhodium complexes through C–H activation: Synthesis, characterization and catalytic activity

Zi-Jian Yao*, Kuan Li, Peng Li, Wei Deng**

School of Chemical and Environmental Engineering, Shanghai Institute of Technology, Shanghai 201418, China

ARTICLE INFO

Article history:
Received 10 May 2017
Received in revised form
20 June 2017
Accepted 22 June 2017
Available online 24 June 2017

Keywords:
Half-sandwich
Iridium
Rhodium
Catalysis

ABSTRACT

A series of mononuclear half-sandwich cyclometalated group 9 (Ir and Rh) metal complexes were synthesized in good yields through metal-mediated C–H bond activation. These air-stable C, N-chelate mode complexes have similar solid state structures. Both experimental results and DFT calculations confirmed that no binuclear complexes were generated in this reaction. The iridium complex **3a** exhibited good catalytic activity for the reduction of both electron-rich and electron-poor aryl imines with low catalyst loading in the presence of formic acid/triethylamine (F/T) azeotropic mixture. All complexes were fully characterized by elemental analysis and IR and NMR spectroscopies. The structures of **1a**, **1b**, **2a**, **3a** and **4b** (see chemical structure formula in Scheme 1 and Scheme 2) were further confirmed by single-crystal X-ray analysis.

1. Introduction

Well-defined metallamacrocycles have attracted considerable interest during the past few years because of their important application in molecular recognition, host-guest chemistry, catalysis, drug delivery and so on [1–10]. Thus the construction of this type of metal supramolecular assembly became one of the most active research fields in coordination chemistry and organometallic chemistry. Different from the preparation of metal-organic frameworks (MOFs) with infinite structure, the coordination number and direction of the metal center need to be controlled for the synthesis of discrete two and three-dimensional metallamacrocycles [11,12]. Large efforts have been paid in this field, and a number of excellent results which using different transition metal compounds as "metal corner" (Pt, Pd, Ir, Rh) have been reported by Raymond [13–15], Stang [16–20], Mirkin [21], Fujita [22–25], and other groups [26–37] in recent years.

Among diverse types of supramolecular coordination complexes, half-sandwich iridium and rhodium ($[Cp^*MCl_2]_2$ (M = Ir, Rh), (*p*-cymene)$RuCl_2$) motif exhibits some particular features in the coordination-driven assembly (Fig. 1) [38,39]: (i) the starting materials can be simply synthesized by the interaction of arene or cyclopentadienyl groups with metal chlorides; (ii) Cp* or substituted benzenes as η^5 or η^6 ligands perfectly shield the potentially octahedral hemisphere of the metals, from which the bonds between the metal and the donor atoms, such as N-, S-, O-, P-donor groups would benefit; (iii) various types of substituents on the cyclopentadienyl ring may be used to tune the solubility and the redox property of the corresponding complexes; (iv) Transition metal complexes with Cp*Ir fragment is one of the most utilized catalysts in water splitting process and often exhibits high catalytic activity [40,41].

On the other hand, ligand choice is also important for the metallamacrocycles construction because they served as the bridge to link the metal corners. Among various types of ligands, aromatic imine ligand has gained major attention in the construction of coordination driven assembly because of their particular features (such as inexpensive, easy to access and air and moisture stable). Systematic work has been done by Jin's group and a series of organoiridium macrocycles have been furnished [38,39]. However, most of the cases have been focused on the *bis*-imine which based on aryl amines. Herein, we explored the reactivity of half-sandwich group 9 compounds with the *bis*-imine ligands based on hydrazine, and a series of mononuclear complexes were afforded. Although the experimental results indicated that the metallamacrocycles could not be formed through this ligand, the obtained mononuclear iridium complexes showed good catalytic activity for the hydrogenation of imines. Additionally, mononuclear complexes were confirmed to be the only products by using DFT study.

* Corresponding author.
** Corresponding author.
E-mail address: zjyao@sit.edu.cn (Z.-J. Yao).

http://dx.doi.org/10.1016/j.jorganchem.2017.06.023
0022-328X/

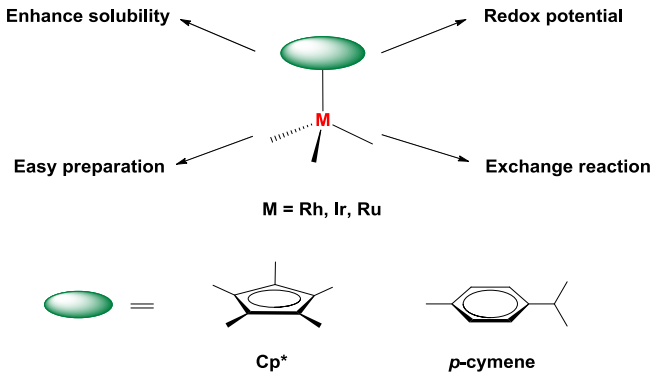

Fig. 1. Properties of half-sandwich complexes.

2. Results and discussion

Schiff base ligands, which are prepared by the condensation reactions of amine and aldehyde, are the one of the simplest and oldest reactions in organic chemistry. Ligands **L1**–**L3** were prepared in high yields by condensation reaction between hydrazine hydrate and two equivalents aromatic aldehydes, according to the classic methods. A few drops of acetic acid were added to the reactions to promote the condensation. With the ligands in hand, we next explored the reactivity of these ligands with one equivalent half-sandwich group 9 metal complexes $[Cp^*MCl_2]_2$ (M = Ir, Rh) in the presence of NaOAc. As shown in Scheme 1, all mononuclear complexes were obtained through *mono* C–H bond activation in moderate to good isolated yields in methanol at elevated temperature. No *bis*-cyclometalated products were found in the reaction. An excess amount of $[Cp^*IrCl_2]_2$ was employed in the reaction to examine whether the *bi*-nuclear complex could be afforded according to the results reported before [42]. However, complex **1a** was still afforded as the only product when the molar ratio of $[Cp^*IrCl_2]_2$ and **L1** increased to 2: 1. Moreover, no new species were observed from the reaction of **1a** with $[Cp^*IrCl_2]_2$ in the presence of NaOAc at 50 °C. The reactions between transition metal precursors and the ligands with either electron-donating or electron-withdrawing groups all afforded the C–H bond activation products smoothly. The mononuclear complexes were also furnished with lower yields by using CH_2Cl_2 as solvent.

The complexes are air and moisture stable in their solid state because of the five-membered chelate rings formation. No decomposition was observed even after heating in toluene for several hours. In addition, TGA measurement of these complexes was conducted to further confirm their thermal stability (see TGA curves in Supporting Information). The results indicate that all the complexes are stable at high temperature (300 °C). They are soluble in toluene and dichloromethane and slightly soluble in diethyl ether and hexane. The obtained mononuclear complexes were fully characterized by various spectroscopic techniques and elemental analysis. The IR spectra of these half-sandwich complexes all display two typical strong and characteristic C=N absorptions at approximately 1620–1500 cm^{-1}, which means that the two C=N are not equivalent and the lower wave numbers are caused by the coordination of the imine nitrogen atom. For complex **1a**, different chemical shift showed at δ 9.19 and 8.59 ppm, which were assigned to the two protons of CH=N groups, also indicated that the metal center only coordinated by one imine group. Six groups of signals in the aromatic region (δ 8.00–7.00 ppm), which were assigned to the protons in the two phenyl rings, indicated the asymmetric structure of **1a**. The analogous single peaks (δ 1.69 (**1a**) and 1.63 (**1b**) ppm) displayed in the ^{1}H NMR spectra of the two complexes suggested identical environments of the Cp* groups. In comparison with the ^{1}H NMR spectrum of **1a**, analogous NMR data of **1b** indicated that the two complexes have similar structures in solution. Similarly, the ^{1}H NMR spectra of **2a**, **b** and **3a**, **b** indicated that all the products are asymmetric mononuclear complexes through one C–H bond activation. The spectroscopic data and elemental analysis of these complexes demonstrate that their structures are similar to each other.

To unambiguously elaborate the structures of these mononuclear half-sandwich complexes, an X-ray analysis is desired. Single crystals suitable for X-ray diffraction analysis were obtained by the slow diffusion of hexane into a saturated solution of them in dichloromethane (Fig. 2). Selected bond lengths and angles are listed in Table 1, and their crystallographic data are summarized in Table 2. Molecular structures of complexes **1a**, **b**, **2a** and **3a** show that the geometry at the metal center is that of a three-legged piano stool with the metal center coordinated by the η^5-Cp* and the C and N atoms, as well as one chloride ligand. The metal center has a distorted-octahedral environment, assuming that the η^5-Cp* group occupies three *fac* coordination sides. The two C=N bond lengths in

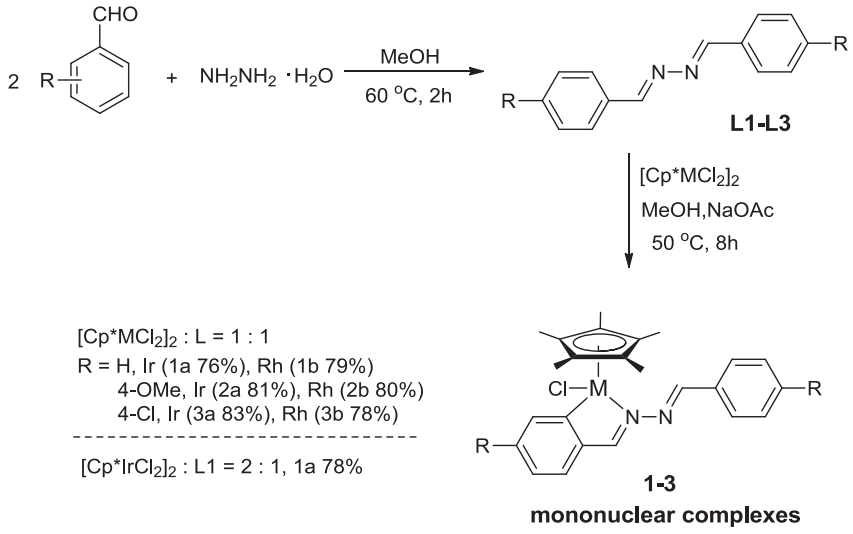

Scheme 1. Synthesis of ligands and mononuclear complexes.

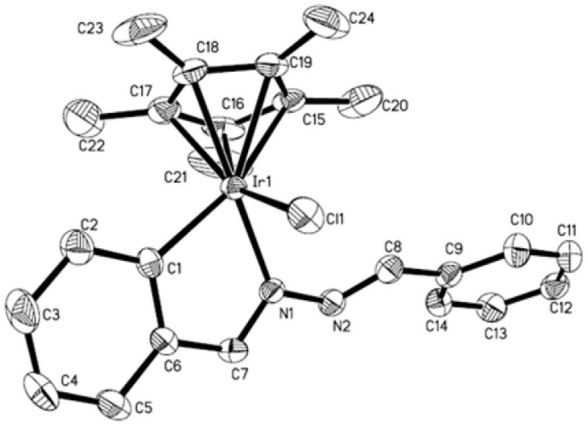

1a

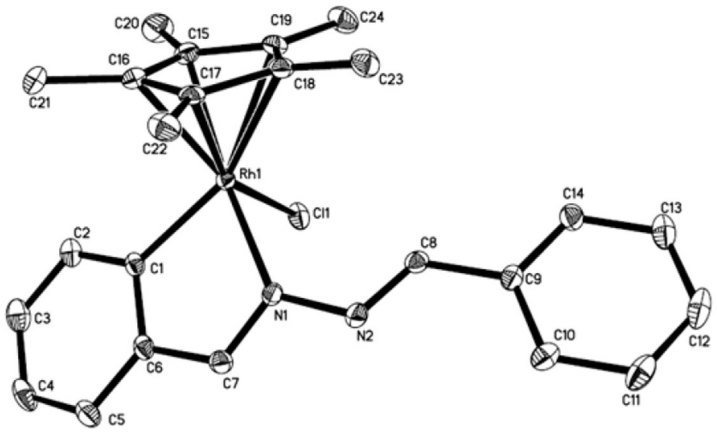

1b

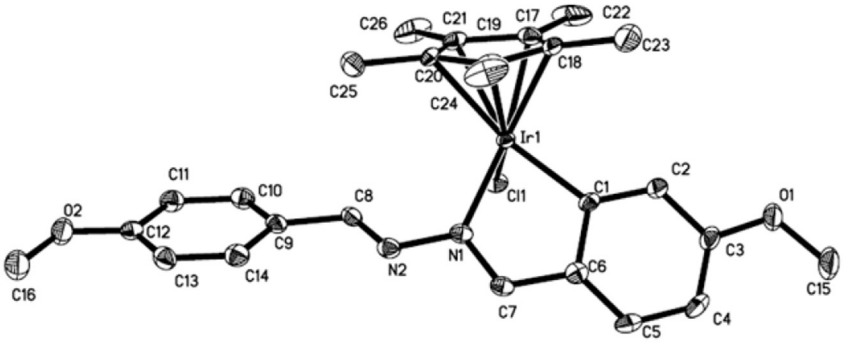

2a

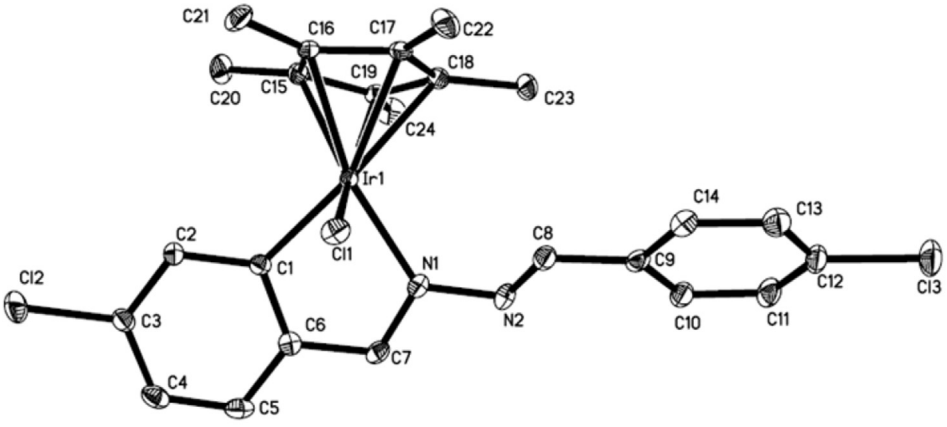

3a

Fig. 2. Molecular structures of **1a**, **1b**, **2a** and **3a** with 30% probability ellipsoids. Hydrogen atoms were omitted for clarity.

all complexes are not equal upon complexes formation revealing coordination of one imine nitrogen atom. The bond lengths of C(7)–N(1) are longer than those of C(8)–N(2) in all complexes, respectively. For complexes **1a** and **1b**, the M–C_{Ph} bond distances of 2.043(4) (1a) and 2.034(2) Å (1b), respectively, which are both within the range of known values for these bonds in analogous complexes [43]. The M–N bond lengths of **1a** and **1b** also compares well with similar bonds found in analogous complexes [42]. The five-membered ring Ir(1)–C(1)–C(6)–C(7)–N(1) of complex **1a** is almost planar with the dihedral angle of 1.7° between planes of N(1)–Ir(1)–C(1) and C(1)–C(6)–C(7)–N(1). The sum of the angles formed by the five-membered ring of 539.9° further confirmed the

Table 1
Crystallographic data and structure refinement parameters for **1a,b**, **2a**, **3a** and **4b**.[a]

	1a	1b	2a	3a	4b
Chemical Formula	$C_{24}H_{26}ClIrN_2$	$C_{24}H_{26}ClRhN_2$	$C_{26}H_{30}ClIrN_2O_2$	$C_{24}H_{24}Cl_3IrN_2$	$C_{24}H_{24}Br_2ClN_2Rh$
FW	570.12	480.83	630.17	639.00	638.63
T/[K]	296(2)	173(2)	173(2)	173(2)	173(2)
λ/Å	0.71073	0.71073	0.71073	0.71073	0.71073
Crystal system	Monoclinic	Monoclinic	Triclinic	Triclinic	Monoclinic
Space group	*P*2(1)/n	*P*2(1)/n	*P*–1	*P*–1	*P*2(1)/c
a/Å	13.8182(14)	7.4677(12)	8.5525(13)	8.3874(8)	7.6606(12)
b/Å	8.1748(8)	16.869(3)	10.9035(17)	10.8102(11)	15.912(2)
c/Å	20.144(2)	17.208(3)	13.423(2)	13.0378(13)	20.022(3)
α/°	90	90	80.809(2)	97.1190(10)	90
β/°	106.070(2)	101.526(2)	87.836(2)	95.250(2)	97.110(3)
γ/°	90	90	77.282(2)	100.2870(10)	90
V/Å^3	2186.6(4)	2124.1(6)	1205.3(3)	1146.3(2)	2421.7(6)
Z	4	4	2	2	4
ρ/Mg m^{-3}	1.732	1.504	1.736	1.851	1.752
μ/mm^{-1}	6.240	0.941	5.675	6.187	4.129
F(000)	1112	984	620	620	1256
θ range/°	2.086–26.945	2.415–26.829	2.279–25.999	1.585–26.998	1.640–27.230
Reflections collected	5870	14414	7763	8007	14688
Completeness to θ	99.3%	99.6%	97.9%	97.5%	99.0%
Data/restraints/param.	4713/30/258	4535/0/258	4654/18/306	4890/0/276	5352/0/276
Goodness-of-fit on F^2	1.069	1.114	1.098	1.111	1.068
Final R indices [I > 2σ(I)[a]]	R1 = 0.0238 wR2 = 0.0681	R1 = 0.0253, wR2 = 0.0753	R1 = 0.0306, wR2 = 0.1190	R1 = 0.0245, wR2 = 0.0728	R1 = 0.0515, wR2 = 0.1594
Largest diff.peak/hole (e Å^{-3})	0.743/–0.618	0.472/–0.410	2.457/–1.908	1.576/–1.610	4.194/–1.084

[a] $R_1 = \Sigma||F_0|-|F_c||/\Sigma|F_0|$ (based on reflections with $F_0^2>2\sigma F^2$). $wR_2 = [\Sigma[w(F_0^2-F_c^2)^2]/\Sigma[w(F_0^2)^2]]^{1/2}$; $w = 1/[\sigma^2(F_0^2)+(0.095P)^2]$; $P = [\max(F_0^2, 0)+2F_c^2]/3$(also with $F_0^2>2\sigma F^2$).

Table 2
Selected bond lengths (Å) and angles (°) for complexes **1a,b**, **2a**, **3a** and **4b.**

Bond lengths (Å) and angles (°)	1a	1b	2a	3a	4b
M(1)–Cl(1)	2.3876(11)	2.4045(7)	2.4017(15)	2.4025(10)	2.4039(15)
M(1)–C(1)	2.043(4)	2.034(2)	2.026(6)	2.048(4)	2.029(6)
M(1)–N(1)	2.085(3)	2.094(2)	2.095(5)	2.090(4)	2.118(5)
C(7)–N(1)	1.291(5)	1.297(3)	1.283(8)	1.306(6)	1.289(8)
C(8)–N(2)	1.255(6)	1.277(3)	1.261(8)	1.277(6)	1.277(8)
N(1)–M(1)–C(1)	76.95(15)	78.12(9)	77.5(2)	77.01(15)	78.2(2)
M(1)–N(1)–C(7)	117.4(3)	115.95(17)	117.6(4)	117.7(3)	115.8(4)
N(1)–C(7)–C(6)	116.0(4)	116.3(2)	116.4(6)	115.2(4)	116.0(6)
C(7)–C(6)–C(1)	114.0(4)	115.0(2)	112.3(5)	114.5(4)	115.3(5)
C(6)–C(1)–M(1)	115.6(3)	114.34(17)	129.1(5)	115.6(3)	114.3(4)

planarity of the cyclemetalated moiety. However, the five-membered ring Rh(1)–C(1)–C(6)–C(7)–N(1) in **1b** is folded with the dihedral angle of 4.7° between planes of N(1)–Rh(1)–C(1) and C(1)–C(6)–C(7)–N(1). The backbone of **2a** and **3a** is very similar to **1a**, including Ir–C_{Ph} and Ir–N bond lengths, and the angles of cyclemetalated rings.

Besides the reactivity study of *para*-substituted ligands with half-sandwich transition metal precursors, interaction between *meta*-substituted ligand **L4** with $[Cp^*MCl_2]_2$ was also investigated. Complexes **4a** and **4b** were afforded under the same reaction condition in 75% and 73% yields, respectively. Theoretically, as shown in Scheme 2, there are two positions available for C–H bond activation. However, from their ^{1}H NMR spectra, complexes **4a** and 4**b** are found to be the only products obtained in the experiment because an important characteristic for the formation of isomers is the splitting of Cp* signals in the ^{1}H NMR spectra (Fig. 3 shows the ^{1}H NMR spectrum of complex **4b**). Complex **4b** crystalized in monoclinic space group *P*2(1)/c and their crystallographic data are summarized in Tables 1 and 2 (Fig. 4). Crystal structure of **4b** indicates that the selective C–H bond activation is probably caused by the steric hindrance [44,45].

The only products of mononuclear complexes (no binuclear complexes was obtained) is clearly of great interest and we have tried to elucidate the reasons using density functional theory

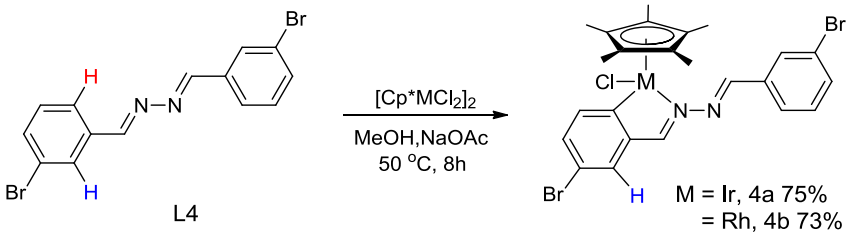

Scheme 2. Selective C–H bond activation of L3.

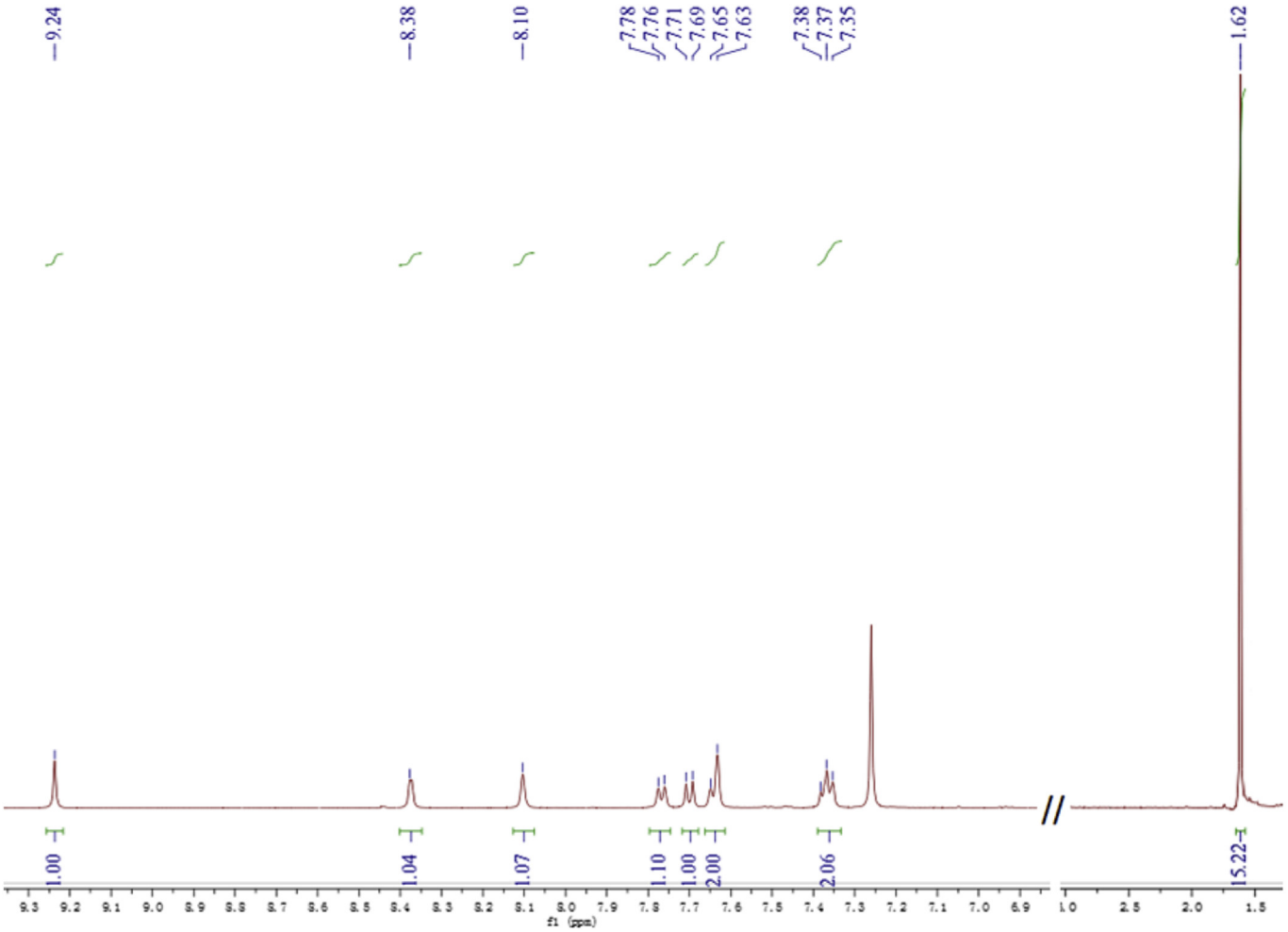

Fig. 3. ^{1}H NMR spectrum of complex **4b**.

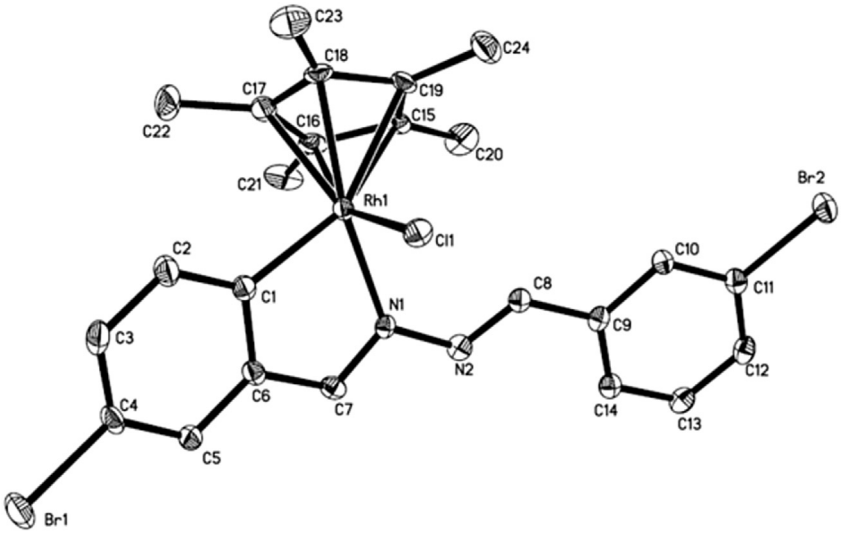

Fig. 4. Molecular structure of **4b** with 30% probability ellipsoids. Hydrogen atoms were omitted for clarity.

calculations (DFT). The energy of the mononuclear iridium complex **1** and binuclear iridium complex **B1** based on **L1** was calculated (Fig. 5). The results obviously show that the energy needed for the formation of **B1** ($\Delta E = 413.80$ kcal/mol) is much higher than that of **M1** ($\Delta E = 16.36$ kcal/mol) at room temperature. So it is reasonable that the binuclear product was not found in the reaction even large

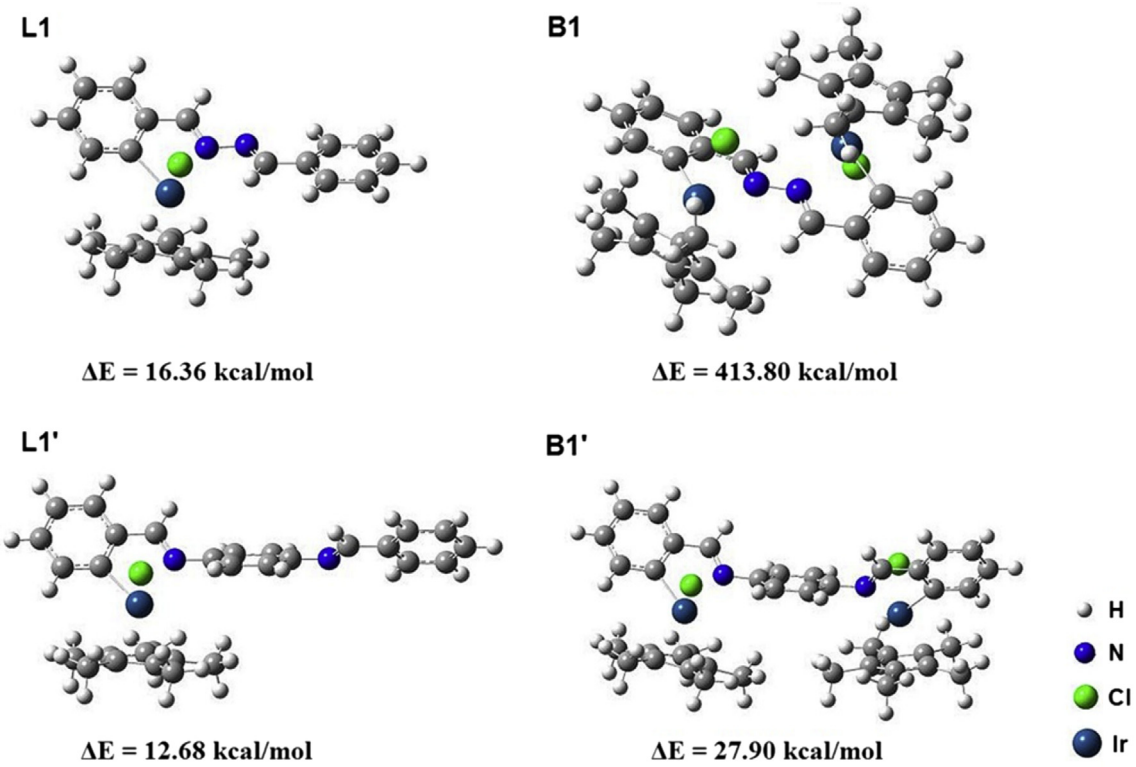

Fig. 5. Computed reaction energy for the formation of **L1**, **L1′**, **B1** and **B1'**.

excess amount of $[Cp^*IrCl_2]_2$ had been employed. The binuclear complex will decompose quickly even if it could be prepared. On the other hand, for the *bis*-imine ligand with a phenyl bridge **L1′**, binuclear iridium complex **B1′** could be obtained because of the slight differences of reaction energy for the formation of **1′** and **B1'** (Fig. 5). The different reactivity between the two ligands (**L1** and **L1′**) is presumably caused by the phenyl bridge which greatly alleviates the steric crowding of the binuclear complex molecule.

The reduction of imines has attracted considerable attention in synthetic chemistry, pharmaceuticals, materials science, and biotechnology [46–51], not only because of the importance of the amine products for the chemical science, but also to the reduction process is the key intermediate of the reductive amination [52]. Compared with the reduction pathway using metal hydride as reducing reagents, catalytic hydrogenation with late transition metal complexes represents a sustainable and green chemical process, crucial for large scale industries. Encouraged by the previous results of the catalytic activity of the iridium complexes [53], we explored the catalytic activity of complexes **1a**–**4a** for the aromatic ketimines to the corresponding ketamines. The hydrogenation reactions were performed in an azeotropic mixture of formic acid/triethylamine (F/T) (serve as H donor) [54] in CF_3CH_2OH using 1 mol% catalyst loading. Preliminary results are summarized in Table 3. Various imine substrates were employed in the reactions and the results demonstrated complexes **1a**-**4a** are indeed catalytic active. Among these iridium catalysts, complex **3a** was found to be the best catalyst for the reaction (Table 3, Entries 1–4). This result indicates that the electron-deficient iridium center is more proper for the catalytic hydrogenation, which is consistent with previous results [52]. Reaction temperature also exhibits influence on the catalytic hydrogenation and 80 °C is proper for the reaction (Table 3, Entries 5 and 6). Decreasing the catalyst loading (0.1 mol%) led to a lower yield of product (Table 3, Entry 3). With the optimized condition in hand, a series of imines were used in the reaction and the results showed that these aryl imines could be reduced to the corresponding amines with high efficiency. Both electron-withdrawing and electron-donating containing substances, whether *ortho*- or *para*-substituted, afforded the corresponding amines in good yields (Table 3, entries 7–12). Scheme 3 shows the proposed mechanism of this reaction. The cyclometalated iridium catalyst reacted with formic acid to generate the iridium hydride through the decarboxylation process. Further interaction between iridium hydride and protonation imine furnished the corresponding amine.

3. Conclusion

A series of mononuclear half-sandwich iridium and rhodium complexes with *bis*-imine ligands based on hydrazine were synthesized through one C–H bond activation. All these transition metal complexes were air- and moisture-stable. DFT calculations further confirmed the experimental results which binuclear complexes could not be generated probably because of the steric crowding. Mononuclear iridium complex **3a** showed good catalytic activity for the reduction of both electron-rich and electron-poor imines with low catalyst loading. The catalytic system exhibited high efficiency and the corresponding amines were given in good yields. Further modification of the ligand and their reactivity study with group 9 metal complexes is currently underway in our lab.

4. Experimental section

4.1. General data

All manipulations were performed under an atmosphere of nitrogen using standard Schlenk techniques. Chemicals were used as

Table 3
Catalytic reduction of imines with iridium complexes **1a**–**4a**.[a]

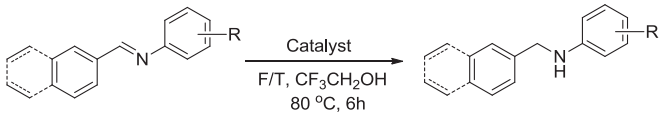

Entry	Catalyst	T/°C	Product	Yield[b]/%
1	**1a**	80	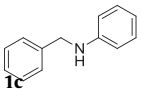 **1c**	76
2	**2a**	80	**1c**	68
3	**3a**	80	**1c**	91/62[c]
4	**4a**	80	**1c**	82
5	**3a**	60	**1c**	81
6	**3a**	90	**1c**	90
7	**3a**	80	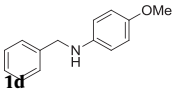 **1d**	92
8	**3a**	80	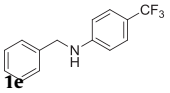 **1e**	88
9	**3a**	80	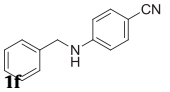 **1f**	89
10	**3a**	80	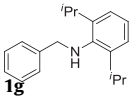 **1g**	82
11	**3a**	80	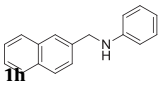 **1h**	88
12	**3a**	80	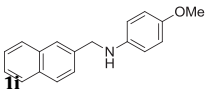 **1i**	87

[a] Reaction conditions: imines (0.5 mmol), catalyst (1 mol%), CF_3CH_2OH (2 mL), F/T (0.5 mL).
[b] Yield was determined by GC analysis, *n*-tridecane was used as internal standard.
[c] 0.1 mol% catalyst was used.

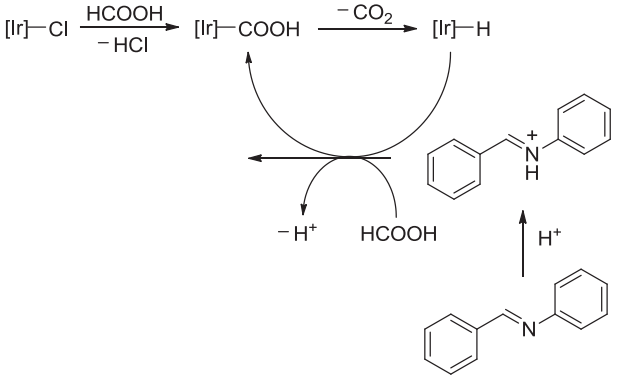

Scheme 3. Propose mechanism of the transfer hydrogenation.

commercial products without further purification. ^{1}H NMR (500 MHz) spectra were measured with a Bruker DMX-500 spectrometer. Elemental analysis was performed on an Elementar vario EL III analyzer. IR (KBr) spectra were measured with the Nicolet FT-IR spectrophotometer.

4.2. Synthesis of bis-imine ligands L1–L4

Hydrazine hydrate (0.25 g, 5.0 mmol) and corresponding aromatic aldehydes (2.5 mmol) were reacted in methanol for 6 h in the presence of catalytic amount of AcOH. Solvent was removed under reduced pressure, and the obtained solid was washing with cold methanol for several times.

L1: yellow solid; 90% yield. ^{1}H NMR (500 MHz, $CDCl_3$, 25 °C): δ 8.69 (s, 2H, CH=N), 7.87–7.85 (m, 4H, Ph), 7.47–7.44 (m, 6H, Ph) ppm. IR (KBr, disk): υ 2943, 1624, 1444, 1306, 1206, 1018, 953, 856, 750 cm^{-1}. Elemental analysis calcd (%) for $C_{14}H_{12}N_2$: C 80.74, H 5.81, N 13.45, found: C 80.67, H 5.85, N 13.59.

L2: yellow solid; 93% yield. ^{1}H NMR (500 MHz, $CDCl_3$, 25 °C): δ 8.61 (s, 2H, CH=N), 7.79 (d, J = 8.5 Hz, 4H, Ph), 6.97 (d, J = 8.5 Hz, 4H, Ph), 3.85 (s, 6H, OMe) ppm. IR (KBr, disk): υ 2925, 1600, 1503, 1297, 1250, 1165, 1021, 832, 617 cm^{-1}. Elemental analysis calcd (%) for $C_{16}H_{16}N_2O_2$: C 71.62, H 6.01, N 10.44, found: C 71.69, H 5.98, N 10.33.

L3: yellow solid; 89% yield. ^{1}H NMR (500 MHz, $CDCl_3$, 25 °C): δ 8.61 (s, 2H, CH=N), 7.79 (d, J = 8.5 Hz, 4H, Ph), 7.44 (d, J = 8.0 Hz, 4H, Ph) ppm. IR (KBr, disk): υ 2943, 1624, 1484, 1399, 1313, 1168, 1088, 861, 819 cm^{-1}. Elemental analysis calcd (%) for $C_{14}H_{10}Cl_2N_2$: C 60.67, H 3.64, N 10.11, found: C 60.74, H 3.63, N 10.16.

L4: yellow solid; 91% yield. ^{1}H NMR (500 MHz, $CDCl_3$, 25 °C): δ 8.57 (s, 2H, CH=N), 8.03 (s, 2H, Ph), 7.73 (d, J = 7.5 Hz, 2H, Ph), 7.60 (d, J = 8.0 Hz, 2H, Ph), 7.34 (t, J = 7.5 Hz, 2H, Ph) ppm. IR (KBr, disk): υ 2951, 1624, 1557, 1463, 1422, 1316, 1205, 1065, 956, 778 cm^{-1}. Elemental analysis calcd (%) for $C_{14}H_{10}Br_2N_2$: C 45.94, H 2.75, N 7.65, found: C 45.82, H 2.63, N 7.56.

4.3. Synthesis of mononuclear complexes 1–4

A mixture of $[Cp^*MCl_2]_2$ (0.1 mmol, M = Ir, Rh), NaOAc (0.6 mmol), and corresponding ligands **L1**–**L4** (0.1 mmol) was stirred at 50 °C in 15 mL of methanol for 8 h. The mixture was filtered and evaporated to give the crude products which were further purified by silica gel column chromatography (CH_2Cl_2: EA = 30: 1) to afford pure cyclometalated mononuclear complexes in yields of 70–85%.

1a: red solid, 76% yield. ^{1}H NMR (500 MHz, $CDCl_3$, 25 °C): δ 9.19 (s, 1H, CH=N), 8.59 (s, 1H, CH=N), 7.90 (d, J = 7.0 Hz, 2H, Ph), 7.85 (d, J = 7.5 Hz, 1H, Ph), 7.59 (d, J = 7.5 Hz, 1H, Ph), 7.51–7.46 (m, 3H, Ph), 7.18 (t, J = 7.5 Hz, 1H, Ph), 7.06 (t, J = 7.0 Hz, 1H, Ph), 1.69 (s, 15H, Cp*) ppm. IR (KBr, disk): υ 2909, 1580, 1528, 1447, 1427, 1209, 1021, 864, 721 cm^{-1}. Elemental analysis calcd (%) for $C_{24}H_{26}ClIrN_2$: C 50.56, H 4.60, N 4.91, found: C 50.62, H 4.63, N 4.88.

1b: red solid, 79% yield. ^{1}H NMR (500 MHz, $CDCl_3$, 25 °C): δ 9.31 (s, 1H, CH=N), 8.45 (s, 1H, CH=N), 7.91 (d, J = 6.0 Hz, 2H, Ph), 7.84 (d, J = 8.0 Hz, 1H, Ph), 7.53–7.48 (m, 4H, Ph), 7.24 (overlapped with $CDCl_3$, 1H, Ph), 7.09 (t, J = 7.0 Hz, 1H, Ph), 1.63 (s, 15H, Cp*) ppm. IR (KBr, disk): υ 2912, 1583, 1531, 1467, 1428, 1213, 1021, 869, 721 cm^{-1}. Elemental analysis calcd (%) for $C_{24}H_{26}ClRhN_2$: C 59.95, H 5.45, N 5.83, found: C 59.88, H 5.36, N 5.91.

2a: red solid, 81% yield. ^{1}H NMR (500 MHz, $CDCl_3$, 25 °C): δ 9.04 (s, 1H, CH=N), 8.48 (s, 1H, CH=N), 7.83 (d, J = 8.5 Hz, 2H, Ph), 7.53 (d, J = 8.5 Hz, 1H, Ph), 7.36 (s, 1H, Ph), 6.98 (d, J = 8.5 Hz, 2H, Ph), 6.62 (d, J = 8.5 Hz, 1H, Ph), 3.90 (s, 3H, OMe), 3.88 (s, 3H, OMe), 1.57 (s, 15H, Cp*) ppm. IR (KBr, disk): υ 2901, 1568, 1512, 1422, 1403, 1191, 1001, 854, 703 cm^{-1}. Elemental analysis calcd (%) for $C_{26}H_{30}ClIrN_2O_2$: C 49.55, H 4.80, N 4.45, found: C 49.58, H 4.73, N 4.49.

2b: red solid, 80% yield. ^{1}H NMR (500 MHz, $CDCl_3$, 25 °C): δ 9.16 (s, 1H, CH=N), 8.33 (s, 1H, CH=N), 7.82 (d, J = 8.5 Hz, 2H, Ph), 7.44 (d, J = 8.5 Hz, 1H, Ph), 7.36 (s, 1H, Ph), 6.98 (d, J = 8.5 Hz, 2H, Ph), 6.62 (d, J = 8.5 Hz, 1H, Ph), 3.90 (s, 3H, OMe), 3.87 (s, 3H, OMe), 1.62 (s,

15H, Cp*) ppm. IR (KBr, disk): υ 2895, 1563, 1510, 1423, 1408, 1196, 1004, 853, 706 cm^{-1}. Elemental analysis calcd (%) for $C_{26}H_{30}ClRhN_2O_2$: C 57.73, H 5.59, N 5.18, found: C 57.82, H 5.65, N 5.21.

3a: red solid, 83% yield. ^1H NMR (500 MHz, $CDCl_3$, 25 °C): δ 9.11 (s, 1H, CH=N), 8.54 (s, 1H, CH=N), 7.83 (d, J = 8.5 Hz, 2H, Ph), 7.76 (s, 1H, Ph), 7.51 (s, J = 8.0 Hz, 1H, Ph), 7.46 (d, J = 8.5 Hz, 2H, Ph), 7.05 (d, J = 8.0 Hz, 1H, Ph), 1.67 (s, 15H, Cp*) ppm. IR (KBr, disk): υ 2906, 1572, 1522, 1430, 1406, 1200, 992, 861, 695 cm^{-1}. Elemental analysis calcd (%) for $C_{24}H_{24}Cl_3IrN_2$: C 45.11, H 3.79, N 4.38, found: C 41.88, H 4.23, N 9.21.

3b: red solid, 78% yield. ^1H NMR (500 MHz, $CDCl_3$, 25 °C): δ 9.24 (s, 1H, CH=N), 8.40 (s, 1H, CH=N), 7.84 (d, J = 8.0 Hz, 2H, Ph), 7.76 (d, J = 3.0 Hz, 1H, Ph), 7.47–7.43 (m, 3H, Ph), 7.07 (d, J = 8.0 Hz, 1H, Ph), 1.62 (s, 15H, Cp*) ppm. IR (KBr, disk): υ 2900, 1555, 1512, 1418, 1399, 1202, 995, 849, 701 cm^{-1}. Elemental analysis calcd (%) for $C_{24}H_{24}Cl_3RhN_2$: C 52.44, H 4.40, N 5.10, found: C 52.36, H 4.33, N 5.18.

4a: red solid, 75% yield. ^1H NMR (500 MHz, $CDCl_3$, 25 °C): δ 9.11 (s, 1H, CH=N), 8.54 (s, 1H, CH=N), 8.10 (s, 1H, Ph), 7.77 (d, J = 7.5 Hz, 1H, Ph), 7.70–7.68 (m, 2H, Ph), 7.65 (d, J = 8.0 Hz, 1H, Ph), 7.37 (t, J = 8.0 Hz, 1H, Ph), 7.28 (overlapped with $CDCl_3$, 1H, Ph), 1.67 (s, 15H, Cp*) ppm. IR (KBr, disk): υ 2918, 1613, 1568, 1429, 1261, 1095, 1027, 803, 633 cm^{-1}. Elemental analysis calcd (%) for $C_{24}H_{24}Br_2ClN_2Ir$: C 39.60, H 3.32, N 3.85, found: C 39.66, H 3.38, N 3.90.

4b: red solid, 73% yield. ^1H NMR (500 MHz, $CDCl_3$, 25 °C): δ 9.24 (s, 1H, CH=N), 8.38 (s, 1H, CH=N), 8.10 (s, 1H, Ph), 7.78 (d, J = 7.5 Hz, 1H, Ph), 7.71 (d, J = 8.0 Hz, 1H, Ph), 7.65–7.63 (m, 2H, Ph), 7.38 (t, J = 7.5 Hz, 1H, Ph), 1.62 (s, 15H, Cp*) ppm. IR (KBr, disk): υ 2912, 1605, 1558, 1421, 1252, 1087, 1022, 793, 643 cm^{-1}. Elemental analysis calcd (%) for $C_{24}H_{24}Br_2ClN_2Rh$: C 45.14, H 3.79, N 4.39, found: C 45.23, H 3.88, N 4.31.

4.4. General procedure for reduction of imines

The substrate imines (0.5 mmol), complex **1a** (1 mol%) were charged in a 10 mL reaction tube with a magnetic bar. The tube was degassed and recharged with nitrogen three times. To the mixture was injected 2 mL CF_3CH_2OH and finally 0.5 mL of $HCOOH/Et_3N$ azeotrope. The resulting mixture was stirred at 80 °C for 6 h. Then the reaction mixture was cooled to room temperature. The resultant mixture was added to an internal standard (*n*-tridecane) to obtain one drop for GC analysis.

4.5. X-ray crystallography

Diffraction data of **1a,b**, **2a**, **3a** and **4b** were collected on a Bruker Smart APEX CCD diffractometer with graphite-monochromated Mo$K\alpha$ radiation (λ = 0.71073 Å). All the data were collected at room temperature, and the structures were solved by direct methods and subsequently refined on F^2 by using full-matrix least-squares techniques (SHELXL) [55]. SADABS [56] absorption corrections were applied to the data, all non-hydrogen atoms were refined anisotropically, and hydrogen atoms were located at calculated positions. All calculations were performed using the Bruker program Smart. A summary of the crystallographic data and selected experimental information are given in Table 1.

Acknowledgements

This work was supported by the National Natural Science Foundation of China (No. 21601125), the Chenguang Scholar of Shanghai Municipal Education Commission (No. 16CG64), Natural Science Foundation of Shanghai (No. 16ZR1435700), the Shanghai Municipal Education Commission (Plateau Discipline Construction Program), Local Institutions Capacity Training of Shanghai Science and Technology Commission, and the Start Funding of Shanghai Institute of Technology (YJ2016-10).

Appendix A. Supplementary data

Supplementary data related to this article can be found at http://dx.doi.org/10.1016/j.jorganchem.2017.06.023.

References

[1] G.F. Swiegers, T.J. Malefetse, Chem. Rev. 100 (2000) 3483–3538.
[2] J.A. Thomas, Chem. Soc. Rev. 36 (2007) 856–868.
[3] N.C. Gianneschi, M.S. Masar, C.A. Mirkin, Acc. Chem. Res. 38 (2005) 825–837.
[4] T.R. Cook, Y.-R. Zheng, P.J. Stang, Chem. Rev. 113 (2013) 734–777.
[5] R. Chakrabarty, P.S. Mukherjee, P.J. Stang, Chem. Rev. 111 (2011) 6810–6918.
[6] T.R. Cook, P.J. Stang, Chem. Rev. 115 (2015) 7001–7045.
[7] M.D. Pluth, R.G. Bergman, K.N. Raymond, Acc. Chem. Res. 42 (2009) 1650–1659.
[8] M. Yoshizawa, J.K. Klosterman, M. Fujita, Angew. Chem. Int. Ed. 48 (2009) 3418–3438.
[9] M. Yoshizawa, M. Tamura, M. Fujita, Science 312 (2006) 251–254.
[10] T.S. Koblenz, J. Wassenaar, J.N.H. Reek, Chem. Soc. Rev. 37 (2008) 247–262.
[11] F.A. Cotton, C. Lin, C.A. Murillo, Acc. Chem. Res. 34 (2001) 759–771.
[12] B.J. Holliday, C.A. Mirkin, Angew. Chem. Int. Ed. 40 (2001) 2022–2043.
[13] D.L. Caulder, R.E. Powers, T.N. Parac, K.N. Raymond, Angew. Chem. Int. Ed. 37 (1998) 1840–1843.
[14] C.J. Brown, G.M. Miller, M.W. Johnson, R.G. Bergman, K.N. Raymond, J. Am. Chem. Soc. 133 (2011) 11964–11966.
[15] W.M. Hart-Cooper, K.N. Clary, F.D. Toste, R.G. Bergman, K.N. Raymond, J. Am. Chem. Soc. 2012 134 (2012) 17873–17876.
[16] V. Vajpayee, Y.H. Song, T.R. Cook, H. Kim, Y. Lee, P.J. Stang, K.-W. Chi, J. Am. Chem. Soc. 133 (2011) 19646–19649.
[17] Y.-R. Zheng, W.-J. Lan, M. Wang, T.R. Cook, P.J. Stang, J. Am. Chem. Soc. 133 (2011) 17045–17055.
[18] B.J. Pollock, T.R. Cook, P.J. Stang, J. Am. Chem. Soc. 134 (2012) 10607–10620.
[19] B.J. Pollock, G.L. Schneider, T.R. Cook, A.S. Davies, P.J. Stang, J. Am. Chem. Soc. 135 (2013) 13676–13679.
[20] Y.-R. Zheng, H.-B. Yang, B.H. Northrop, K. Ghosh, P.J. Stang, Inorg. Chem. 47 (2008) 4706–4711.
[21] M.J. Wiester, P.A. Ulmann, C.A. Mirkin, Angew. Chem. Int. Ed. 50 (2011) 114–137.
[22] D. Fujita, A. Takahashi, S. Sato, M. Fujita, J. Am. Chem. Soc. 133 (2011) 13317–13319.
[23] M. Yoneya, T. Yamaguchi, S. Sato, M. Fujita, J. Am. Chem. Soc. 134 (2012) 14401–14407.
[24] Y. Fang, T. Murase, S. Sato, M. Fujita, J. Am. Chem. Soc. 135 (2013) 613–615.
[25] M. Yoshizawa, J.K. Klosterman, M. Fujita, Angew. Chem. Int. Ed. 48 (2009) 3418–3438.
[26] M.M.J. Smulders, S. Zarra, J.R. Nitschke, J. Am. Chem. Soc. 135 (2013) 7039–7046.
[27] J.L. Iliger, A.M. Belenguer, J.R. Nitschke, Angew. Chem. Int. Ed. 52 (2013) 7958–7962.
[28] A. Granzhan, C. Schouwey, T. Riis-Johannessen, R. Scopelliti, K. Severin, J. Am. Chem. Soc. 133 (2011) 7106–7115.
[29] F. Schmitt, J. Freudenreich, N.P.E. Barry, L. Juillerat-Jeanneret, G. Süss-Fink, B. Therrien, J. Am. Chem. Soc. 134 (2012) 754–757.
[30] A. Garci, J.-P. Mbakidi, V. Chaleix, V. Sol, E. Orhan, B. Therrien, Organometallics 34 (2015) 4138–4146.
[31] A.-P. Barry, N.P.E. Barry, V. Russo, B. Heinrich, B. Donnio, B. Therrien, R. Deschenaux, J. Am. Chem. Soc. 136 (2014) 17616–17625.
[32] F.M. Conrady, R. Frohlich, C. Schulte to Brinke, F.E. Hahn, J. Am. Chem. Soc. 133 (2011) 11496–11499.
[33] Y.-F. Han, G.-X. Jin, F.E. Hahn, J. Am. Chem. Soc. 135 (2013) 9263–9266.
[34] S.-L. Huang, Y.-J. Lin, T.S.A. Hor, G.-X. Jin, J. Am. Chem. Soc. 135 (2013) 8125–8128.
[35] B. Sun, M. Wang, Z. Lou, M. Huang, C. Xu, X. Li, L.-J. Chen, Y. Yu, G.L. Davis, B. Xu, H.-B. Yang, X. Li, J. Am. Chem. Soc. 137 (2015) 1556–1564.
[36] L.-J. Chen, G.-Z. Zhao, B. Jiang, B. Sun, M. Wang, L. Xu, J. He, Z. Abliz, H. Tan, X. Li, H.-B. Yang, J. Am. Chem. Soc. 136 (2014) 5993–6001.
[37] Z.Y. Li, Y. Zhang, C.W. Zhang, L.-J. Chen, C. Wang, H. Tan, Y. Yu, X. Li, H.-B. Yang, J. Am. Chem. Soc. 136 (2014) 8577–8589.
[38] Y.-F. Han, G.-X. Jin, Acc. Chem. Res. 47 (2014) 3571–3579.
[39] Y.-F. Han, G.-X. Jin, Chem. Soc. Rev. 43 (2014) 2799–2823.
[40] M.D. Kärkäs, O. Verho, E.V. Johnston, B. Åkermark, Chem. Rev. 114 (2014) 11863–12001.
[41] J.M. Thomsen, D.L. Huang, R.H. Crabtree, G.W. Brudvig, Dalton Trans. 44 (2015) 12452–12472.
[42] L. Zhang, H. Li, L.-H. Weng, G.-X. Jin, Organometallics 33 (2014) 587–593.
[43] W.-B. Yu, Y.-F. Han, Y.-J. Lin, G.-X. Jin, Organometallics 30 (2011) 3090–3095.
[44] L. Li, W.W. Brennessel, W.D. Jones, Organometallics 28 (2009) 3492–3500.

[45] A.P. Walsh, W.D. Jones, Organometallics 34 (2015) 3400–3407.
[46] S. Gomez, J.A. Peters, T. Maschmeyer, Adv. Synth. Catal. 344 (2002) 1037–1057.
[47] A.F. Abdel-Magid, S.J. Mehrman, Org. Process Res. Dev. 10 (2006) 971–1031.
[48] T.C. Nugent, M. El-Shazly, Adv. Synth. Catal. 352 (2010) 753–819.
[49] R.P. Tripathi, S.S. Verma, J. Pandey, V.K. Tiwari, Curr. Org. Chem. 12 (2008) 1093–1115.
[50] K.S. Hayes, Appl. Catal. A 221 (2001) 187–195.
[51] J.M. Antos, M.B. Francis, Curr. Opin. Chem. Biol. 10 (2006) 253–262.
[52] C. Wang, A. Pettman, J. Bacsa, J. Xiao, Angew. Chem. Int. Ed. 49 (2010) 7548–7552.
[53] J. Talwar, D. Wu, S. Johnston, M. Yan, J. Xiao, Angew. Chem. Int. Ed. 52 (2013) 6983–6987.
[54] S. Hashiguchi, A. Fujii, J. Takehara, T. Ikariya, R. Noyori, J. Am. Chem. Soc. 117 (1995) 7562–7563.
[55] G.M. Sheldrick, SHELXL-97, Program for the Refinement of Crystal Structures, Universität Gtötingen, Germany, 1997.
[56] G.M. Sheldrick, SADABS (2.01), Bruker/Siemens Area Detector Absorption Correction Program, Bruker AXS, Madison, WI, 1998.